COBEM 2021 26th International Congress of Mechanical Engineering
November 22-26, 2021, Virtual Congress, Brazil

COB-2021-0219
Breakup of two-layer liquid films

Pedro Calderano
Marcio Carvalho
Pontifical Catholic University of Rio de Janeiro
msc@puc-rio.br

Abstract. *Thin liquid sheets are present in a variety of systems and applications, including curtain coating process. One of the most important process limits is the curtain breakup, which sets a lower limit for the coating liquid flow rate. Consequently, this lower limit flow rate defines the minimum possible thickness of the deposited film. Experimental evidences have shown that using a two-layer curtain with a highly viscoelastic thin layer may delay the curtain breakup, allowing coating of thinner films. The optimization of the two-layer curtain process with the goal of reducing the minimum flow rate is not fully understood. In the present work, we study the breakup of two-layer liquid sheets, composed of a Newtonian and a viscoelastic liquid, by solving the set of differential equations that describe this free boundary problem. The model is derived from the basic hydrodynamic equations using a longwave approximation and the resulting set of differential equation is solved by the finite difference method. We investigate the effect of different process parameters and liquid properties on the breakup time. The results show how the viscoelastic forces delay the breakup, stabilizing the liquid sheet.*

Keywords: *non-Newtonian fluid, viscoelastic fluid, thin film, curtain coating, double-layered sheets*

1. INTRODUCTION

Liquid coating is a manufacturing process used to enhance the functionality and quality of products. Thin-film layers increase and modify the functionality of a substrate by protecting surfaces from wear, improving lubricity, improving corrosion resistance, providing chemical resistance, and many other functions (Martin (2009)). Among the several coating processes, this study will concentrate on the process known as curtain coating. In curtain coating process, a liquid sheet is formed as the liquid exits the die and flows downwards in the form of a liquid curtain, before impinging the moving substrate. Eventually, small wave-form perturbations will appear on the sheet's free surfaces. These disturbances may either evolve by increasing their amplitude until their size is large enough to breakup the sheet or be dissipated, leading to curtain maintenance. The mentioned sheet breakup will lead to a defect in the fabrication process, which validates the search for a better understanding of this phenomenon.

The evolution of surface configuration on thin liquid films has been a field of study for different applications such as coatings, adhesives, flotation, and biological membranes (Oron *et al.* (1997)),(Bandyopadhyay *et al.* (2005)). Therefore, thin films have been investigated in a variety of conditions, such as on a substrate (Pototsky *et al.* (2004)) and in between substrates (Merkt *et al.* (2005)). These films are susceptible to small perturbations on their surface since the interface between the liquid and the surrounding gas is a deformable boundary (Oron *et al.* (1997)). Brown (1961) reported that the stability of a liquid curtain depends on the flow rate of coating material passing through the slot die. Additionally, he established a limit criteria by balancing a force proportional to the curtain's momentum with the surface tension force.

The breakup process knowledge has been explored to meet aspirations of boosting coating speed and reducing the thickness of the liquid film (Karim *et al.* (2020)) without hole formation and maintaining uniform thickness. In this regard, Erneux and Davis (1993) considered the Navier-Stokes equations for free films to derive its long-wave evolution equation and found a bifurcation point from where the stability of a curtain may be inferred. The proposed stability threshold only take into account surface tension and van der Waals forces. Following this work, Ida and Miksis (1996) developed a numerical simulation to estimate the sheet rupture time, from a small amplitude perturbation to the sheet pinch-off. Among recent advances, Becerra and Carvalho (2011) experimentally shows the violation of Brown's rule (Brown (1961)) by the manipulation of viscosity using complex fluids. Stable and thinner liquid curtain is possible when the extensional viscosity effects of the coating polymer solution are strong. Marston *et al.* (2014) also presented an experimental investigation on the breakup of liquid curtains. The authors explored single and multi-layer sheets and showed that the established rule for the minimum flow rate is valid for all sheets examined. Still, the hysteresis window varied with the number of layers in the sheet.

Bazzi and Carvalho (2019) extended the Erneux and Davis (1993) stability indicator analysis, showing it is also accurate for complex fluids. Besides, the work shows the effect of viscoelastic stress on sheet rupture dynamics. Viscoelastic

forces can significantly delay the breakup moment on unstable sheets when compared with the breakup time of Newtonian fluids.

Karim *et al.* (2020) experimentally showed that two-layer sheets remained stable at significantly thinner thicknesses than single-layer sheets. Karim compared a double-layer curtain composed of a shear-thinning fluid bottom layer and a viscoelastic fluid top layer to a single-layer curtain constituted by a shear-thinning layer. The double-layer sheet was much thinner, depending on fluid properties. The authors acknowledge the viscoelastic top layer as the main factor contributing to the perturbation growth diminish and consequently to the thickness reduction reported.

In this work, we aim to numerically model the breakup process of double-layered sheets and determine a relationship between viscosity characteristics and layer thicknesses, and rupture time. The results can be used to design two-layer curtain coating processes that enable the delay of sheet breakup to thinner curtains, allowing thin coatings.

The remainder of this paper is organized as follows. Section 2. presents the mathematical model; Section 3. introduces the linear stability analysis; Section 4. addressees the numerical results; and Section 5. states our main conclusions regarding the proposal.

2. MATHEMATICAL MODEL

It is considered a two-layered film system with external free surfaces, as sketched in Fig. 1a. The mathematical model developed to describe the curtain composed of assembled layers is two-dimensional with a thickness dimension, z, and a length dimension, x, passing along one of the free surfaces, as sketched in Fig. 1b. Figure 1b represents the coordinated system adopted in this work.

The system is derived from the mass and momentum conservation equations, given by

$$\nabla \cdot \mathbf{u}_i = 0, \tag{1}$$

and

$$\rho \frac{D}{Dt}\mathbf{u}_i = \nabla \cdot \mathbf{T}_i + \nabla \mathbf{\Phi_i}, \tag{2}$$

where i indicates the sheet layer, $i = \{1, 2\}$ ($i = 1$ denotes the lower layer, while $i = 2$ denotes the upper layer), $\mathbf{u}$ stands for the velocity vector, ρ represents the fluid density, $\mathbf{T}$ is the stress tensor, and $\mathbf{\Phi}$ the van der Waals potential, which is defined as

$$\Phi = \frac{A}{h^3}, \tag{3}$$

where A is the Hamaker constant, which in this case relates two boundary sheets through a medium (coating fluid). h represents the layer thickness. As we have two layers, h is divided into h_1 and h_2, which are respectively the thickness of the bottom layer and the total sheet thickness. Hence, the Eq. (3) is written as

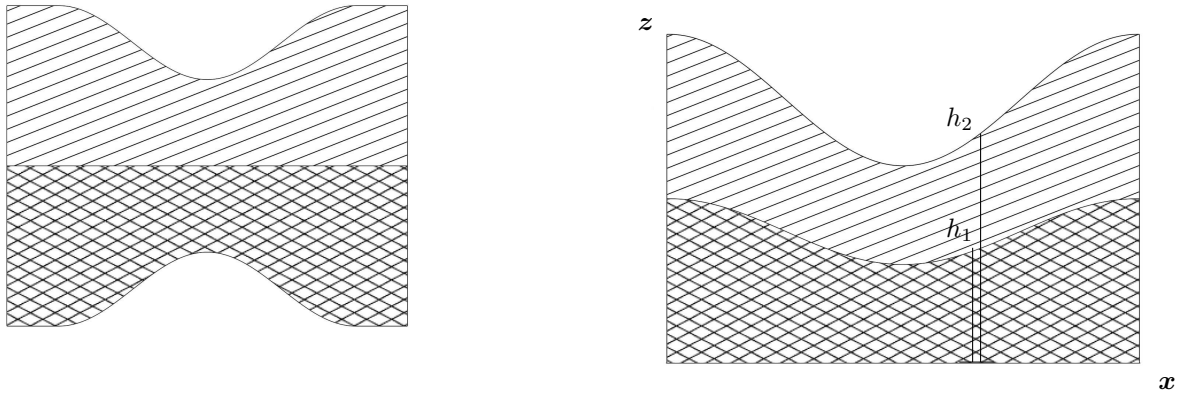

(a) (b)

Figure 1. Representation of the bilayer that composes the fluid sheet. In (a), the image shows the actual system configuration. In (b), the image shows the adopted shifted coordinate system.

$$\Phi_1 = \frac{A_{01}}{h_1^3}, \tag{4}$$

for the bottom layer, and for the upper layer we have

$$\Phi_2 = \frac{A_{02}}{(h_2 - h_1)^3}. \tag{5}$$

The van der Waals potential among the external surfaces is not considered.

The normal and tangential forces balance are taken as boundary conditions. The unit normal and tangential vectors are defined as

$$\boldsymbol{n} = \left[\frac{\partial h}{\partial x}; \quad -1\right]\left(1 + \left(\frac{\partial h}{\partial x}\right)^2\right)^{-1/2}, \; and \quad \boldsymbol{t} = \left[1; \quad \frac{\partial h}{\partial x}\right]\left(1 + \left(\frac{\partial h}{\partial x}\right)^2\right)^{-1/2}, \tag{6}$$

where $\boldsymbol{n}_i$ and $\boldsymbol{t}_i$ are the normal and tangential vectors respectively. h corresponds to the layer surface height in the z-axis. Due to sheet slenderness, the approximation $(\partial h/\partial x)^2 \longrightarrow 0$ is adopted.

The boundary conditions on the top of the second layer at $z = h_2$ are written as:

$$\boldsymbol{n_2} \cdot \boldsymbol{\tau} \cdot \boldsymbol{n_2} = \sigma\kappa \Longrightarrow -p_2 + \tau_{zz2} - 2\tau_{xz2}\frac{\partial h_2}{\partial x} = \sigma\kappa, \tag{7}$$

and

$$\boldsymbol{t_2} \cdot \boldsymbol{\tau} \cdot \boldsymbol{n_2} = 0 \Longrightarrow \frac{\partial h_2}{\partial x}\left(\tau_{xx2} - \tau_{zz2}\right) - \tau_{zx2} = 0. \tag{8}$$

u and v represents components of the velocity vector $\overline{u}$ in the $x-$ and $z-$ direction. σ is surface tension and κ stands for the surface curvature.

Again, the boundary conditions between the two layers layer, at $z = h_1$, are written as:

$$\boldsymbol{n_2} \cdot \boldsymbol{\tau} \cdot \boldsymbol{n_2} = \boldsymbol{n_1} \cdot \boldsymbol{\tau} \cdot \boldsymbol{n_1} \Longrightarrow -\left(p_1 - p_2\right) + \left[\tau_{zz1} - 2\tau_{zx1}\frac{\partial h_1}{\partial x}\right] - \left[\tau_{zz2} - 2\tau_{zx2}\frac{\partial h_2}{\partial x}\right] = 0, \tag{9}$$

and

$$\boldsymbol{t_1} \cdot \boldsymbol{\tau} \cdot \boldsymbol{n_1} = \tau = K\left(u_1 - u_2\right) \Longrightarrow \frac{\partial h_1}{\partial x}\left(\tau_{xx1} - \tau_{zz1}\right) - \tau_{zx1} = K\left(u_1 - u_2\right). \tag{10}$$

K stands for the ratio of the fluid viscosities; $K = \mu_2/\mu_1$.

Lastly, there is the kinematic condition, Equation (11), which syncs surface movement and velocity.

$$\boldsymbol{n}_i \cdot \boldsymbol{u}_i = \left(\frac{\partial h_i}{\partial t}\right) \Longrightarrow \frac{\partial h_i}{\partial t} + u_i\frac{\partial h_i}{\partial x} = v_i. \tag{11}$$

A long-wave approximation is adopted in the system development. This approximation expands the variables through an asymptotic expansion, as done before to study single layer liquid films (Bazzi and Carvalho (2019)),(Stewart *et al.* (2015)),(Savva and Bush (2009)). Variables that are symmetric with respect to z-direction are expanded as:

$$\phi_i\left(x, z, t\right) = \phi_0^{\textcircled{i}} + \phi_2^{\textcircled{i}} z^2 + ..., \tag{12}$$

where ϕ expresses the expanded variable. Variables that are not symmetric to the $z-$axis, they are expanded as

$$\phi_i\left(x, z, t\right) = \phi_1^{\textcircled{i}} z + \phi_3^{\textcircled{i}} z^3 + ... \tag{13}$$

Due to the thin thickness of the layers, $z \ll 1$, higher-order z terms are truncated as the equations are developed. Also, we perform the simplification $z \longrightarrow h(x)$ to the remaining terms that are multiplied by z, since this long-wave supposes plug flow and the forces acting on the system, besides viscous forces, depend on the sheet's thickness.
It is adopted $(\partial h/\partial x)^2 \longrightarrow 0$, $z^2 \longrightarrow 0$, and $\kappa \approx \partial^2 h_2/\partial x^2$. Lastly, it is necessary to consider a constitutive model stress tensor equation. Here, it is adopted the upper-convected Oldroyd-B model (Irgens (2014)).

$$\boldsymbol{\tau} + \lambda \boldsymbol{\tau}^{\boldsymbol{\nabla}} = \eta \dot{\boldsymbol{\gamma}}, \tag{14}$$

where $\dot{\boldsymbol{\gamma}}$ is the strain rate tensor, and the convective derivative is defined as

$$\boldsymbol{\tau}^{\boldsymbol{\nabla}} = \frac{D}{Dt}\boldsymbol{\tau} - \boldsymbol{\nabla}\mathbf{u} \cdot \boldsymbol{\tau} - \boldsymbol{\tau} \cdot \boldsymbol{\nabla}\mathbf{u}. \tag{15}$$

Then, the stress tensor is applied and the equations in the system are further developed. Subsequently, the dimensional variables are substituted by non-dimensional variables, based as the appropriate scales, defined as

$$U^* = U\frac{\rho_2 L}{\mu_2}, \quad t^* = t\frac{\mu_2}{L^2\rho_2}, \quad h^* = \frac{h}{H}, \quad x^* = \frac{x}{L}, \quad \tau^* = \tau\frac{\rho^2 L}{\mu_2^2},$$

in which L refers to sheet length and H to sheet thickness. From now on, all variables displayed are dimensionless, therefore, we hide the * symbol. After the system development, we finally come to the system of coupled PDEs:

$$\frac{\partial h_1}{\partial t} + U^{①}\frac{\partial h_1}{\partial x} + h_1\frac{\partial U^{①}}{\partial x} = 0 \tag{16}$$

$$\begin{aligned}
&\frac{\partial U^{①}}{\partial t} + U^{①}\frac{\partial U^{①}}{\partial x} - 3S_1\frac{\partial^3 h_2}{\partial x^3} - 4D\frac{\partial^2 U^{①}}{\partial x^2} - 4D\frac{1}{h_1}\frac{\partial h_1}{\partial x}\frac{\partial U^{①}}{\partial x} - \\
&- E\left(\frac{\partial \tau_{xx}^{①}}{\partial x} - \frac{\partial \tau_{zz}^{①}}{\partial x}\right) - E\frac{1}{h_1}\frac{\partial h_1}{\partial x}\left(\tau_{xx}^{①} - \tau_{zz}^{①}\right) + 2k\frac{\partial^2 h_1}{\partial x^2}\left(U^{①} - U^{②}\right) + \\
&+ 2k\frac{\partial h_1}{\partial x}\left(\frac{\partial U^{①}}{\partial x} - \frac{\partial U^{②}}{\partial x}\right) + \mathbb{L}\frac{1}{h_1}\left(U^{①} - U^{②}\right) - \frac{3}{16}A_1\frac{1}{h_1^4}\frac{\partial h_1}{\partial x} = 0
\end{aligned} \tag{17}$$

$$\frac{\partial h_2}{\partial t} + U^{②}\frac{\partial h_2}{\partial x} + h_2\frac{\partial U^{②}}{\partial x} = 0 \tag{18}$$

$$\begin{aligned}
&\frac{\partial U^{②}}{\partial t} + U^{②}\frac{\partial U^{②}}{\partial x} - 3S_2\frac{\partial^3 h_2}{\partial x^3} - 4\frac{\partial^2 U^{②}}{\partial x^2} - 4\frac{1}{h_2}\frac{\partial h_2}{\partial x}\frac{\partial U^{②}}{\partial x} - L\left(\frac{\partial \tau_{xx}^{②}}{\partial x} - \frac{\partial \tau_{zz}^{②}}{\partial x}\right) - \\
&- L\frac{1}{h_2}\frac{\partial h_2}{\partial x}\left(\tau_{xx}^{②} - \tau_{zz}^{②}\right) - \frac{3}{16}A_2\frac{1}{(h_2 - h_1)^4}\left(\frac{\partial h_2}{\partial x} - \frac{\partial h_1}{\partial x}\right) = 0
\end{aligned} \tag{19}$$

$$De\frac{\partial \tau_{xx}}{\partial t} = -\tau_{xx} - De\,u\frac{\partial \tau_{xx}}{\partial x} + 2De\,\frac{\partial u}{\partial x}\tau_{xx} + 2\eta_r\frac{\partial u}{\partial x} \tag{20}$$

$$De\frac{\partial \tau_{zz}}{\partial t} = -\tau_{zz} - De\,u\frac{\partial \tau_{zz}}{\partial x} - 2De\,\frac{\partial u}{\partial x}\tau_{zz} - 2\eta_r\frac{\partial u}{\partial x} \tag{21}$$

in which

$$S_1 = \frac{\sigma H\rho_2^2}{6\mu_2^2\rho_1}, \qquad S_2 = \frac{\sigma H\rho_2}{6\mu_2^2}, \qquad A_1 = \frac{A_{01}\rho_2^2 L^2}{6\pi H^3\mu_2^2\rho_1}, \qquad A_2 = \frac{A_{02}\rho_2 L^2}{6\pi H^3\mu_2^2},$$

$$D = \frac{\mu_1\rho_2}{\rho_1\mu_2}, \qquad E = \frac{\rho_2 L}{\rho_1}, \qquad k = \frac{K\rho_2 H}{\rho_1\mu_2}, \qquad \mathbb{L} = \frac{K\rho_2 L^2}{H\rho_1\mu_2}, \qquad De = \frac{\lambda\eta_s}{L^2\rho_2},$$

are the dimensionless coefficients. The model response recovers a Newtonian fluid when the non-Newtonian non-dimensional parameters are set as $\eta_r = 0$ and $De = 0$.

3. LINEAR STABILITY ANALYSIS

Linear stability analysis is a valuable tool used to infer whether the sheet is stable or not. Previous works have presented the analysis for single-layer systems (Erneux and Davis (1993)),(Bazzi and Carvalho (2019)). Here we develop stability analysis considering a viscoelastic double-layer sheet. This analysis will be important to ensure the initial conditions of the numerical procedure are properly tuned.

The analysis is developed through a perturbation in a steady-state solution in the system of equations presented in Eqs. (16)-(21). The steady-solution assumes null fluid velocity, constant stress tensor, and constant surface configuration in both layers. The perturbation changes the steady-state solution, making it flow in a stable or unstable pattern depending on fluid conditions. The solution of the transient problem is written as the sum of the steady state solution plus a time-dependent perturbation:

$$\begin{aligned}\left(h_2, U^{②}, \tau_{xx}^{②}, \tau_{zz}^{②}\right) &= \left(\overline{h_2} + h_2',\ 0 + u_2',\ 0 + \tau_{xx2}',\ 0 + \tau_{zz2}'\right),\\ \left(h_1, U^{①}, \tau_{xx}^{①}, \tau_{zz}^{①}\right) &= \left(\overline{h_2}\mathcal{H} + h_1',\ 0 + u_1',\ 0 + \tau_{xx1}',\ 0 + \tau_{zz1}'\right).\end{aligned} \tag{22}$$

The factor $\mathcal{H}$ is a constant that the relationship between the initial layers $\#1$ and $\#2$ heights, so $\mathcal{H} = h_1/\left(h_2 - h_1\right)$. As stated, the steady-state solution is unchanging, then the mean values are

$$\left(\overline{h_2},\ \overline{h_2}\mathcal{H}\right) = \left(0.5,\ 0.5\mathcal{H}\right). \tag{23}$$

The perturbation added in this solution follow the expressions

$$\begin{aligned}\left(h_2', u_2', \tau_{xx2}', \tau_{zz2}'\right) &= \left(h_{02}, u_{01}, \tau_{xx01}, \tau_{zz01}\right)\delta exp(\omega t + i\alpha x),\\ \left(h_1', u_1', \tau_{xx1}', \tau_{zz1}'\right) &= \left(h_{01}, u_{02}, \tau_{xx02}, \tau_{zz02}\right)\delta exp(\omega t + i\alpha x),\end{aligned} \tag{24}$$

where δ indicates the small amplitude of the perturbation in comparison to the variable mean value, $\delta \ll 1$. This small amplitude leads to suppression of higher order terms, i.e. $\delta^2 \to 0$. The position x is restricted to the bounded space domain $x \in \mathbb{R}/-1 < x < 1$ and the wavenumber is established as $\alpha = n\pi$, where n may take natural numbers excluding zero (Erneux and Davis (1993)). The perturbation variable ω is the growth rate, which indicates how the perturbation evolves with time. The perturbation amplitude grows if $\omega > 0$ or reduces with time progression if $\omega < 0$. When $\omega = 0$, the perturbation is not affected by time. Therefore, we shall isolate the term ω to analyze how the system behaves and point out which parameters influence system stability. Proceeding, the proposed solution relations presented by Eq. (22) are used on the developed viscoelastic system of equations.

Using the relations presented in the Eqs. (23) and (24) in the system we get

$$\begin{aligned}&\omega^2 + \frac{3S}{2}\left(1+\mathcal{H}\right)\alpha^4 + 4D\alpha\omega + \frac{4E\eta_r\alpha^2\omega}{1+De\omega} + \frac{2L}{\mathcal{H}}\frac{u_{01}-u_{02}}{u_{01}}\omega - 6\frac{A_1}{\mathcal{H}^3}\alpha^2 = 0,\\ &\omega^2 + \frac{3S}{2}\left(1+\mathcal{H}\right)\alpha^4 + 4\alpha\omega + \frac{4L\eta_r\alpha^2\omega}{1+De\omega} - 6A_2\alpha^2 = 0.\end{aligned} \tag{25}$$

Those relations are related to the first and second layers, respectively. From them, as the system is stable for $\omega <= 0$, the stability criteria shows that the first layer of the curtain is stable when

$$\frac{S}{A_1} >= \frac{4}{\pi^2\left(1+\mathcal{H}\right)\mathcal{H}^3}, \tag{26}$$

and the second layer is stable when

$$\frac{S}{A_2} >= \frac{4}{\pi^2\left(1+\mathcal{H}\right)}. \tag{27}$$

4. RESULTS

4.1 Solution method

The equation system, Eqs. (16)-(21), was discretized in space using second-order finite difference approximation in a central finite difference scheme. Following Bazzi and Carvalho (2019) and Savva and Bush (2009), it was adopted in

this work a unidimensional staggered grid. The nodes associated with the u and τ variables are placed in the between of h related nodes, in a way that h_i is computed at x_i, while u_i and τ_i are computed at $(x_i + x_{i+1})/2$. The mesh covers the $0 \leq x \leq L$ interval, which comprehends from the section where the minimum cross-sectional area is placed to the perturbation end. Time discretization was done using an implicit Cranck-Nicholson method (Ferziger *et al.* (2002)). We adopted Newton's method to solve the non-linear system at each time step (Ferziger *et al.* (2002)).

Concerning initial conditions, the velocity and stress vectors, $\boldsymbol{u}_i^0$, $\boldsymbol{\tau}_{xx_i}^0$ and $\boldsymbol{\tau}_{zz_i}^0$, are initially arrays of zeros. It assumes that the fluid is not moving in any particular direction. The vector which represents the surfaces, $\boldsymbol{h}_i^0$, are initialized with the addition of a height value plus a small deviation, so it is possible to observe how the system evolves from this perturbed configuration. This starting deviation is a cosine wave, where the deviation amplitude is $\epsilon_0 = 2\%$ of the sheet's height.

4.2 Validation

The model validation was conducted by comparing the predictions obtained for a single layer sheet with results presented in the literature. The time evolution of the liquid sheet was compared with the results presented by Bazzi and Carvalho (2019). As previous works studied the evolution of single-layer sheets, the validation was performed using the same fluid parameters for both layers. This validation examines the temporal thickness evolution and compares the proposed model behavior to the behavior of reference works. Hence, the proposed model must show similar sheet surface progress to be considered correctly implemented. The progress analysis is performed comparing the rupture times achieved by the proposed models and the values reported by Bazzi and Carvalho (2019). Considering the minimum thickness on the sheet profile over time, Figure 2a exhibits that the Oldroyd-B proposed model recovers literature behavior concerning the perturbation evolution. Regarding the models in broad circumstances, Fig. 2b compares the proposed model to Bazzi and Carvalho (2019) model rupture times for different fluid parameters. Figure 2b compares the Oldroyd-B model rupture times for multiple η_r and De values. As these values increase, the non-Newtonian fluid characteristic gets stronger. It is perceptible that fluids with a stronger non-Newtonian nature have a further delay in rupture time.

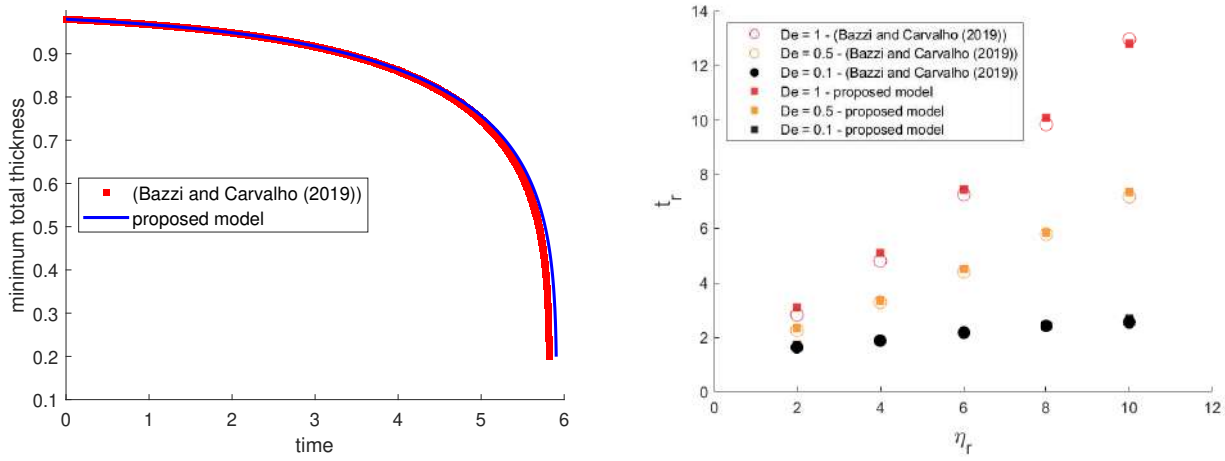

(a) (b)

Figure 2. Images presenting validation data. (a) Graphical comparison of minimum total thickness in the sheet profile over time among the (Bazzi and Carvalho (2019)) Oldroyd-B model and the proposed Oldroyd-B model, where the fluid parameters are $\eta_r = 8$ and $De = 0.5$. The proposal recovers the behavior described in the literature for the perturbation evolution. (b) Graphical comparison of rupture times among the (Bazzi and Carvalho (2019)) Oldroyd model and the proposed Oldroyd model. The proposal recovers the literature rupture times, t_r, effectively.

4.3 Linear stability investigation

Concerning the exhibited linear stability, the system is simulated throughout a range of different values in the ratio among surface tension and van der Waals potential. In these simulations, the two-layer sheets have equal fluid parameters for both layers. The results show agreement with the determined limit criteria developed.

The stability check is performed using the auxiliary constant γ, defined as

$$\gamma = \frac{S/A}{S/A_{cr}}, \tag{28}$$

where S/A_{cr} is the critical value for the S/A ratio. Using this constant on the stability analysis result, Eqs. (26) and

(27), it is explored a range of S/A ratios. Therefore, according to the Eq. (28), the sheet should be stable for $\gamma > 1$ and unstable for $\gamma < 1$.
Figure 3 shows the sheet stability over a range of γ. The change in perturbation amplitude indicates sheet stability. It is shown the perturbation amplitude change from $t = 0$ to $t = 0.5$. Change in perturbation amplitude is computed as $\Delta\epsilon = \epsilon\,(t = 0.5) - \epsilon_0$ since ϵ is the deviation from the the mean profile thickness. Stability occurs when $\gamma > 1$ since this is the range where $\Delta\epsilon < 0$, indicating the decrease in wave amplitude. Analogously, the curtain is unstable for $\gamma < 1$. It is also noticeable, as reported in Bazzi and Carvalho (2019), that as viscoelastic effects become stronger, the modulus of change in amplitude for a given period decreases. It indicates that viscoelastic effects do not change the critical parameters for flow stability but slows down the growth of the perturbation.

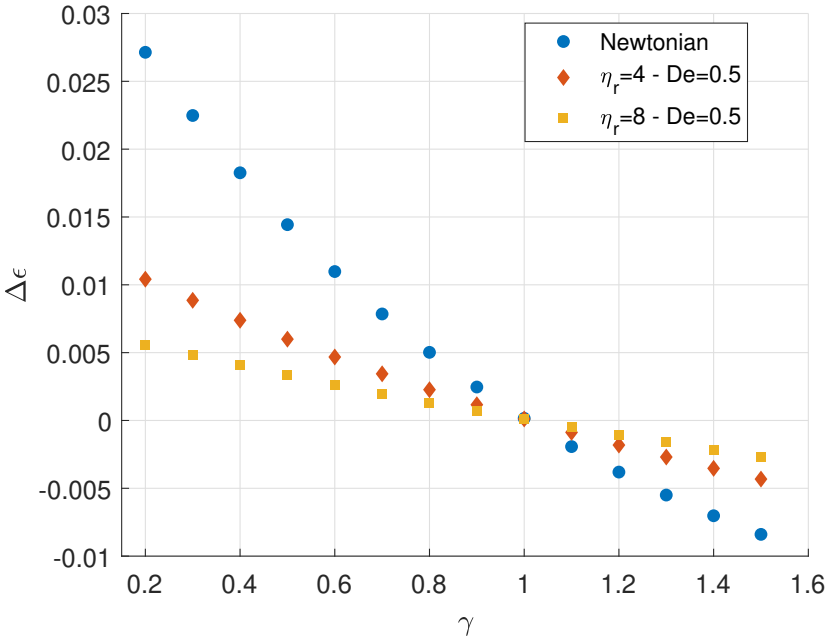

Figure 3. Change in perturbation amplitude over a range of γ from $t = 0$ to $t = 0.5$. $\Delta\epsilon$ is computed as $\Delta\epsilon = \epsilon\,(t = 0.5) - \epsilon_0$. Curtain is stable when $\Delta\epsilon < 0$, and unstable when $\Delta\epsilon > 0$.

4.4 Sheet surface evolution

We investigate curtains constituted by two layers with different fluid properties and analyze the curtain time evolution. We also vary the layer thickness ratio to obtain a broader perspective on the subject.

First, we analyze sheets constituted by two layers of Newtonian fluids. The fluid density is the same in both layers. The second layer viscosity is fixed as $\mu_2 = 1$ mPa.s, and for the first layer, viscosity, μ_1, is a factor multiplied by the viscosity μ_2. The non-dimensional thicknesses are initialized using the relationship $\mathcal{H}$ that defines the ratio between the thickness of the two layers at the initial time, $\mathcal{H} = h_1/\,(h_2 - h_1)$. So, these heights are initialized as $h_1 = 0.5\mathcal{H}$ and $h_2 = 0.5\,(1 + \mathcal{H})$. The ratio between the non-dimensionals of capillary and van der Waals forces are set according to $S_1/A_1 = 2/\left(\pi^2\,(1 + \mathcal{H})\,\mathcal{H}^3\right)$ and $S_2/A_2 = 2/\left(\pi^2\,(1 + \mathcal{H})\right)$, therefore the curtain is unstable since $\gamma < 1$.

Here it is considered the surface evolution of double and single-layered sheets. As the sheets are initialized with different non-dimensional thickness ratios, $\mathcal{H}$, it is performed a normalization before the sheet profile analysis.

$$\begin{aligned} h_{1norm} &= h_1/\,(0.5\,(1 + \mathcal{H}))\,, \\ h_{2norm} &= h_2/\,(0.5\,(1 + \mathcal{H}))\,. \end{aligned} \tag{29}$$

This normalization aids the comparisons among different sheets since the normalized minimum height for the upper layer always starts at the height of $1 - \epsilon_0$. Figure 4 presents the evolution of the normalized values of minimum height with time considering the perturbation profile of a two-layer sheet and a single-layer sheet. The former is constituted by a Newtonian and a viscoelastic Oldroyd-B layer ($\eta_r = 4$, $De = 0.5$), while the latter is formed only by the Newtonian liquid layer ($\mu = 1$ mPa.s). Figure 4 shows that the thin non-Newtonian layer stabilizes the sheet and extends the demanded time to rupture. The thin viscoelastic extra layer slows down the thickness reduction since the beginning of the perturbation evolution. Then, the extra viscoelastic layer delays the breakup moment.

Figure 5 shows the velocity profile in the last point in time for the Newtonian–Oldroyd-B sheet in both layers. The modulus of the velocity profile difference goes to zero when compared to the velocity, $\mathcal{O}(-3)$ and $\mathcal{O}(1)$ respectively. Although the difference between velocity profiles in the different layers is small, it produces shear stress values, Eq. (10), high enough to maintain the evolution of both layers coupled.

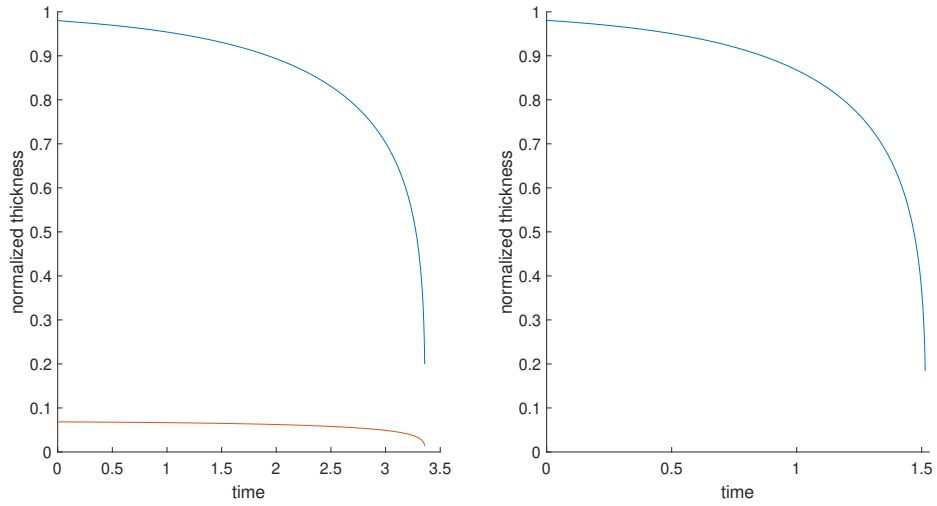

Figure 4. Normalized minimum thickness over time. On the left, a sheet constituted by a thick Newtonian layer and a thin viscoelastic layer with the fluid properties $\eta_r = 4$, $De = 0.5$, and $\mathcal{H} = 0.15$. On the right, a single sheet of Newtonian fluid, $\mu = 1$ mPa.s.

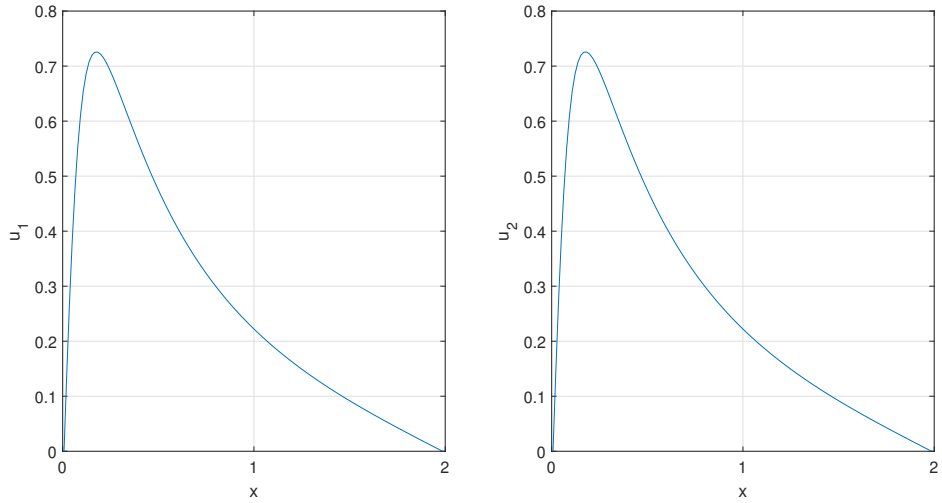

Figure 5. Velocity profile in the entire sheet length when the sheet is about to pinch-off. The sheet is constituted by a Newtonian layer and a viscoelastic layer with the fluid properties $\eta_r = 4$, $De = 0.5$, and $\mathcal{H} = 0.15$.

4.5 Curtain thickness reduction

The results presented previously by Karim *et al.* (2020) show experimentally that it is possible to reduce the sheet thickness of a curtain when a single layer sheet is substituted by a double layer sheet with one thin viscoelastic layer. It is exploited in this subsection the curtain thickness reduction numerically. We have indicated that the addition of an extra thin layer of a viscoelastic liquid delays the rupture moment in an unstable sheet. Then, it is computed the achievable curtain thickness reduction based on this delay. It is simulated the sheet thickness reduction for different values of γ, presented in Equation (28), and different viscoelastic forces, characterized by η_r. From the definition of the non-dimensional coefficient, the ratio S/A may be expressed as

$$\frac{S}{A} = \frac{\sigma H^4 \pi}{A_0 L^2}, \tag{30}$$

in which H is the dimensional sheet thickness. Therefore, the variation in γ represents different sheet thickness since the σ, A_0, and L remain constant. Then, higher γ indicates the curtain is thicker. First, it is simulated the rupture time of Newtonian single layers for each of the S/A ratios to be used as a reference. Then, we compute the rupture time for double sheets composed of Newtonian–viscoelastic layers with reduced thickness. The dimensional thickness reduction, H reduction, is performed by multiplying into the γ the value $(1-\zeta)^4$, see Equation (30), where ζ is the percentage reduction in dimensional thickness. Sheet rupture happens when the rupture time is shorter than the perturbation residence time on the curtain. The maximum reduction possible is calculated, ζ_{max}, considering the reference rupture time. As stated in previous Subsections, the addition of an extra viscoelastic layer delays the sheet breakup time. So, this time buffer to the rupture moment can be leveraged by reducing the curtain thickness. Therefore, ζ_{max} is defined when the double layer system rupture time matches the reference single sheet rupture time. Figure 6 shows the results for maximum reduction percentage for all cases. We found that for higher S/A ratios, the potential reduction in sheet thickness is fainter. In a physical setting, the need for higher S/A ratios may be related to lengthier sheets, since disturbances that appear on the sheet surface take longer to get to the sheet's end. On the other hand, the increase in the non-Newtonian fluid viscoelasticity increases the maximum value for possible thickness reduction. Karim *et al.* (2020) found experimentally the same behavior regarding the viscoelastic effects reported.

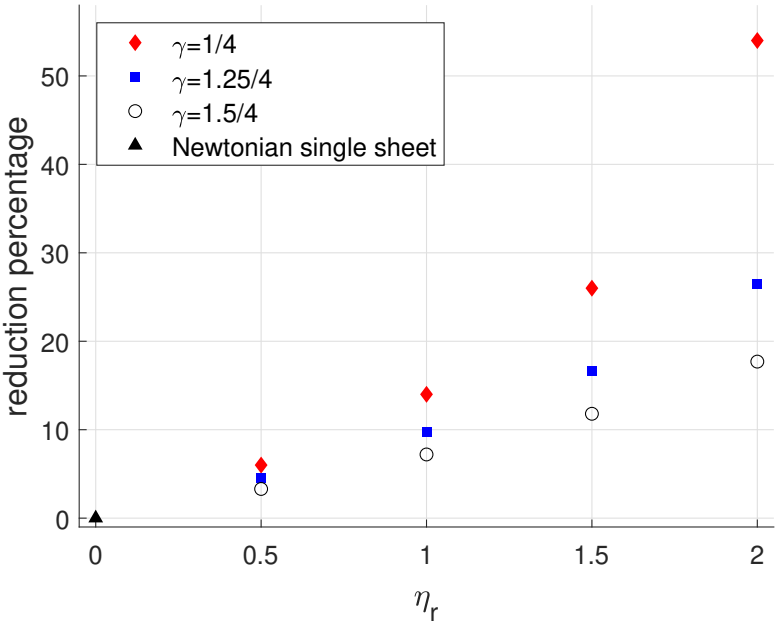

Figure 6. Reduction percentage on the dimensional thickness varying the γ and η_r parameters. The De parameter is set as a constant $De = 0.25$. The thickness of a single-layered Newtonian sheet is considered for reference, $\mu = 1$ mPa.s. The reduction bases on a comparison between the reference and the value for a viscoelastic-Newtonian double layer.

5. CONCLUSION

We numerically studied the development of two-layer sheets under unstable conditions until their rupture. The model applied investigates two-layer sheets in different layer thickness ratios. It was examined as double-layers in which the sheet was composed of a Newtonian layer and a thin viscoelastic layer. Considering the rupture time of a Newtonian single layer sheet, the results show extended rupture times for double-layered sheets when one of its layers is viscoelastic. Finally, it is performed simulations on dimensional thickness reduction based on the addition of a viscoelastic second layer. Those results reveal the effects of viscoelasticity and curtain length variation on the maximum sheet thickness reduction achievable.

6. ACKNOWLEDGEMENTS

This work was supported by the Coordenação de Aperfeiçoamento de Pessoal de Nível Superior - Brasil (CAPES) - Finance Code 001. We also thank the Carlos Chagas Filho Research Support Foundation (FAPERJ, E-26/200.260/2020). Any opinions, findings, conclusions, or recommendations expressed here are those of the authors and do not necessarily reflect the views of the sponsors.

7. REFERENCES

Bandyopadhyay, D., Gulabani, R. and Sharma, A., 2005. "Instability and dynamics of thin liquid bilayers". *Industrial & engineering chemistry research*, Vol. 44, No. 5, pp. 1259–1272.

Bazzi, M. and Carvalho, M., 2019. "Effect of viscoelasticity on liquid sheet rupture". *Journal of Non-Newtonian Fluid Mechanics*, Vol. 264, pp. 107–116.

Becerra, M. and Carvalho, M.S., 2011. "Stability of viscoelastic liquid curtain". *Chemical Engineering and Processing: Process Intensification*, Vol. 50, No. 5-6, pp. 445–449.

Brown, D., 1961. "A study of the behaviour of a thin sheet of moving liquid". *Journal of fluid mechanics*, Vol. 10, No. 2, pp. 297–305.

Erneux, T. and Davis, S.H., 1993. "Nonlinear rupture of free films". *Physics of Fluids A: Fluid Dynamics*, Vol. 5, No. 5, pp. 1117–1122.

Ferziger, J.H., Perić, M. and Street, R.L., 2002. *Computational methods for fluid dynamics*, Vol. 3. Springer.

Ida, M.P. and Miksis, M.J., 1996. "Thin film rupture". *Applied Mathematics Letters*, Vol. 9, No. 3, pp. 35–40.

Irgens, F., 2014. *Rheology and non-newtonian fluids*, Vol. 190. Springer.

Karim, A.M., Suszynski, W.J., Pujari, S., Francis, L.F. and Carvalho, M.S., 2020. "Delaying breakup and avoiding air entrainment in curtain coating using a two-layer liquid structure". *Chemical Engineering Science*, Vol. 213, p. 115376.

Marston, J., Thoroddsen, S.T., Thompson, J., Blyth, M.G., Henry, D. and Uddin, J., 2014. "Experimental investigation of hysteresis in the break-up of liquid curtains". *Chemical Engineering Science*, Vol. 117, pp. 248–263.

Martin, P.M., 2009. *Handbook of deposition technologies for films and coatings: science, applications and technology*. William Andrew.

Merkt, D., Pototsky, A., Bestehorn, M. and Thiele, U., 2005. "Long-wave theory of bounded two-layer films with a free liquid–liquid interface: short-and long-time evolution". *Physics of Fluids*, Vol. 17, No. 6, p. 064104.

Oron, A., Davis, S.H. and Bankoff, S.G., 1997. "Long-scale evolution of thin liquid films". *Reviews of modern physics*, Vol. 69, No. 3, p. 931.

Pototsky, A., Bestehorn, M., Merkt, D. and Thiele, U., 2004. "Alternative pathways of dewetting for a thin liquid two-layer film". *Physical Review E*, Vol. 70, No. 2, p. 025201.

Savva, N. and Bush, J.W., 2009. "Viscous sheet retraction".

Stewart, P.S., Feng, J., Kimpton, L.S., Griffiths, I.M. and Stone, H.A., 2015. "Stability of a bi-layer free film: simultaneous or individual rupture events?" *Journal of Fluid Mechanics*, Vol. 777, pp. 27–49.

8. RESPONSIBILITY NOTICE

The authors are solely responsible for the printed material included in this paper.